Acid−Base Equilibria in Rhodopsin: Dependence of the Protonation State of Glu134 on Its Environment†

Xavier Periole,* Marc A. Ceruso,* and Ernest L. Mehler

Department of Physiology and Biophysics, Box 1218, Mount Sinai School of Medicine, One Gustave L. Levy Place, New York, New York 10029

Received January 6, 2004; Revised Manuscript Received March 23, 2004

ABSTRACT: Glutamic acid E134 in rhodopsin is part of a highly conserved triad, D(E)RY, located near the cytoplasmic lipid/water interface in transmembrane helix 3 of G protein-coupled receptors (GPCRs). A large body of experimental evidence suggests that the protonation of E134 plays a role in the mechanism of activation of rhodopsin and other GPCRs as well. For E134 to change its protonation state, its pK_a value must shift from values below physiological pH to higher values. Because of the proximity of the triad to the lipid/water interface, it was hypothesized that a change in solvent around E134 from water to lipid could induce such a shift in pK_a. To test this hypothesis, the pK_a values of the titratable amino acid residues in rhodopsin have been calculated and the change in solvent around E134 was modeled by shifting the position of the lipid/water interface. The approach used to carry out the pK_a calculations takes into account the partial immersion of transmembrane proteins in lipid. Qualitative experimental evidence is available for several residues regarding their likely protonation state in rhodopsin at or near physiological pH. Comparison of the calculated pK_a values with these experimental findings shows good agreement between the two. Notably, glutamic acids E122 and E181 were found to be protonated. The pK_a values were then calculated for a range of lipid/water interface positions. Although the surrounding solvent of several titratable residues changed from water to lipid in this range, leading to pK_a shifts in most cases, only for E134 would the shift lead to a change in protonation state at physiological pH. Thus, our results show that the protonation state of E134 is particularly sensitive to its environment. This sensitivity together with the location of E134 near the actual position of the lipid/water interface could be a strategic element in the mechanism of activation of rhodopsin.

Rhodopsin belongs to the largest family of G protein-coupled receptors (GPCRs), the class I or rhodopsin-like GPCRs. GPCRs are integral membrane proteins involved in signal transduction across the cell plasma membrane in processes as diverse as vision, taste, olfaction, and neurotransmission. GPCRs share a common 7-helix bundle organization that comprises the transmembrane domain (TMD), as exhibited by the crystal structure of the visual pigment rhodopsin (*1*).

The mechanism of activation of rhodopsin is the best characterized among GPCRs, and many techniques have been developed and refined to detect rhodopsin photoproducts (*2*, *3*). On exposure to light, the 11-*cis*-retinal chromophore that is bound to K296 inside the TMD isomerizes to all-*trans*-retinal. During this isomerization, a number of photoproducts [photo, batho, blue shifted intermediate, lumi, meta I, and meta II (MII)], distinguished both by spectroscopic and structural properties, have been characterized (*2*, *4*−*6*). These photoproducts accompany a structural relaxation cascade that ultimately leads to the formation of the active state of rhodopsin, MII. The formation of MII is marked by a conformational change that involves, in particular, the disruption of the cytoplasmic side of the interface between transmembrane helix (TMH)-3 and TMH-6 (*7*). MII is the form of rhodopsin that binds the G protein transducin (Gt) (*2*). MII exists in temperature- and pH-dependent equilibrium with the still inactive precursor metarhodopsin I (MI) (*8*). In addition to the deprotonation of the Schiff base, the transition from MI to MII involves the uptake of one (*9*) or more (*10*, *11*) protons and is accompanied by protonation changes of key opsin residues (*11*). Among these, E113 and E181 are noteworthy because they have been shown to play the role of counterions to the protonated Schiff base K296 (PBS) in rhodopsin (*12*, *13*) and MI (*14*), respectively. Moreover, E113 is the Schiff base proton acceptor in MII (*12*). D83 is also of interest because it has been shown to be protonated in rhodopsin and to change its hydrogen-bonding network upon activation (*15*). Finally, E134 is of particular interest because it is part of the conserved D(E)RY triad (E134, R135, and Y136 in rhodopsin) in TMH-3 (*16*) near the lipid/water interface on the cytoplasmic side (see below).

Considerable evidence exists for a role of E134 in the MI/MII equilibrium in rhodopsin. E134 was shown to become protonated in MII upon Gt binding (*17*−*19*), and the E134Q mutant has been shown to displace the MI/MII equilibrium toward MII (*11*, *20*) and to abolish the pH dependence of the MI/MII equilibrium and the uptake of two protons (*11*).

† The work was supported in part by NIH Grants P01 DA12923 and R01 DA15170.

* To whom correspondence should be addressed. (M.C.) E-mail: mceruso@physbio.mssm.edu. (X.P.) Current address: Department of Biophysical Chemistry (GBB), University of Groningen, Nijenborgh 4, 9747 AG Groningen, The Netherlands. E-mail: x.periole@chem.rug.nl.

10.1021/bi049949e CCC: $27.50
Published on Web 05/11/2004

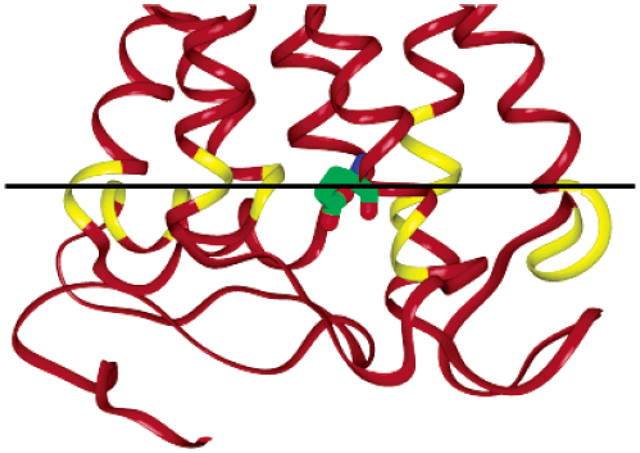

FIGURE 1: Cytoplasmic lipid/water interface in rhodopsin. The lipid/water interface is defined as the border between the hydrophobic region of the lipid from the polar headgroups. The cytoplasmic termini of rhodopsin's TMHs are shown as ribbons. E134 is shown in stick representation. The line indicates the position of the lipid/water interface determined by Stenkamp et al. (*28*). This line corresponds to the L− line in Figure 2. The position of the lipid/water interface determined by Khorana and co-workers (*27*, *68*−*70*) is shown in yellow.

It has been suggested as well that the E134Q mutant adopts a local active-like conformation even in the dark (*21*). Analogous behavior is observed in other GPCRs, where mutation of the acidic residue in the position corresponding to E134 increases basal activity (*22*−*26*). Thus, although there is no direct evidence for the protonation of E134 in the MII state without Gt, E134 is the most likely candidate for the proton uptake observed upon rhodopsin activation (*11*).

To become protonated, the pK_a of E134 must shift to values greater than the local (physiological) pH. One way that such a shift could be realized is for the microenvironment around the residue to become more hydrophobic on activation. Such a mechanism has been suggested on the basis of experimental findings (*19*). Here, we propose that a key determinant in this process may be the position of the E134 relative to the lipid/water interface surrounding rhodopsin. We define the lipid/water interface as the border between the hydrophic region of the lipids and the polar headgroups, e.g., we include the polar headgroups in the water medium (see Materials and Methods). On the basis of electron paramagnetic resonance studies of spin-labeled single cysteine mutants of rhodopsin in dodecyl maltoside, Khorana and co-workers place the cytoplasmic side of the lipid/water interface for TMH-3 between residues V137 and V138, i.e., one helical turn below E134 (*27*). According to these results, E134 lies within the membrane bilayer region, quite likely near the border between the polar headgroups and the hydrophobic region. In contrast, a more recent study (*28*), which analyzes the distribution of residue properties in the structure of rhodopsin along the membrane normal axis, places the cytoplasmic lipid/water interface slightly above the position of the E134 side chain, thereby putting E134 in the solvent phase. These findings suggest that the position of the lipid/water interface is not clearly defined (Figure 1).

To test the hypothesis that the protonation of E134 is particularly affected by its position relative to the hydrophobic region of the membrane, the pK_a values of all of the titratable residues in rhodopsin were first calculated and then the effect of moving the lipid/water interface on both sides of rhodopsin was evaluated. The microenvironment modulated-screened Coulomb potential (MM-SCP) approach (*29*, *30*) is used to calculate the pK_a values. The original method has been modified to take into account the presence of the membrane embedding the protein (see Materials and Methods). Here, it is shown that the protonation state predicted from the calculated pK_a values is in good agreement with the available experimental data. We also show that when the side chain of E134 changes from being below the lipid/water interface (within the water region) to being above it (embedded in the lipid region), we observe a substantial increase of the overall hydrophobicity of its local environment leading to a large shift of its pK_a value.

MATERIALS AND METHODS

Electrostatic Calculations. Formulation of the MM-SCP algorithm has been described in detail elsewhere (*30*). Briefly, the pK_a values of the protonatable residues in a protein are calculated relative to a reference state by employing a standard thermodynamic cycle (*31*, *32*). Thus, the pK_a for group A in the protein is given by

$$pK_a^A(p) = pK_a^A(s) + (w_A^{int} + \Delta w_A^{tr\prime})/2.303RT \qquad (1)$$

where $pK_a^A(p)$ and $pK_a^A(s)$ are the pK_a values of group A in the protein and solvent, respectively, w_A^{int} represents the electrostatic interaction free energy of group A in the field of all of the other residues in the protein, and $\Delta w_A^{tr\prime} = \alpha_A \Delta w_A^{tr}$ is the net change in the self-energy between residue A immersed in water and in the protein, which is itself embedded in water. α_A is a linear scaling factor that models the effects of transferring a titratable group into a very hydrophobic local environment (*33*). The treatment of internal waters as part of the continuum and the values of the scaling factor, α_A, were described previously (*33*). The problem of calculating the pK_a values reduces to evaluating the interaction and transfer energies and the linear scaling parameter. The calculation of the energy terms is based on a screened Coulomb potential, where the distribution of the titration charge over the titratable moiety is determined variationally to optimize the total electrostatic free energy (*29*).

Microenvironments. The inhomogeneity of proteins is a key determinant of their properties (*34*−*36*) and has been shown to play an important modulating role on pH-dependent electrostatic properties (*33*). To incorporate these effects into an algorithm for calculating pK_a values, it is necessary to have a set of quantitative descriptors for characterizing the observed inhomogeneity. The approach that has been developed assumes that the primary determinant of inhomogeneity important for electrostatic effects in proteins is the degree of hydrophobicity or hydrophilicity (denoted here by Hpy) of the local environment (microenvironment) around the titratable group. The microenvironment around a group is defined as the volume swept out by a 4.25 Å sphere placed on every nonhydrogenic atom belonging to the group. Any atom or fragment from neighboring amino acid residues (or other chemical entities) within this volume contributes to the Hpy value of the microenvironment evaluated from its

Table 1: Hydrophobicity of Microenvironment of Titratable Groups in Octane and Water[a]

residue	titratable group[b]	Hpy^o	Hpy^w
His	C−imidazole	6.015	−18.453
Lys	C−NH_3	3.758	−11.420
Arg	C(NH)C(NH_2)$_2$	7.106	*d*
Tyr	C−OH	3.325	−8.368
Asp	C−COO	5.127	−13.492
Glu	C−COO	4.634	−12.832
Lyr	C−NH=CH	*c*	

[a] Hpy^o = octane values; Hpy^w= water values. [b] Moiety of the titratable residue that carries the charge as defined in CHARMM PAR19 (*41*). [c] Hpy of the Schiffs base titratable moiety set to Lys value. [d] Not calculated, set to Lys value.

Rekker hydrophobic fragmental constant [Table 2 in ref *30* gives the assignments of the Rekker coefficients (*37*, *38*) used in the MM-SCP algorithm]. It is calculated from:

$$\mathrm{Hpy_A} = \sum_{a}^{N_A} \sum_{b}^{N_B} d_b \,\mathrm{RFHC}_b \quad (r_{ab} \le 4.25\ \text{Å}), (\mathrm{B} \neq \mathrm{A}) \quad (2)$$

where RFHC$_b$ is the fragmental hydrophobic constant of atom *b* in group B, N_A and N_B are the number of atoms in groups A and B, respectively, and $d_b = 1$ if atom *b* has not been counted or 0 if it has been counted, so that each atom's contribution is counted only once. Equation 2 defines the protein's contribution to the hydrophobicity/hydrophilicity of the microenvironment, but it does not contain any information regarding the degree of burial of the group or any contribution from the accessible solvent. Both of these descriptors can be incorporated by defining the quantity

$$\mathrm{THpy_A} = (1 - \xi_A)\mathrm{Hpy_A} + \xi_A \mathrm{Hpy_A^s} \quad (3)$$

In eq 3, THpy is the total hydrophobicity of the microenvironment around the fragment, ξ_A is the solvent-exposed fraction, and Hpy$_A^s$ is the contribution of the solvent to THpy$_A$, where the superscript represents the pure solvent. Neither Hpy nor THpy are normalized and therefore are not suitable for comparing groups in different microenvironments. A normalized quantity is given by

$$\mathrm{rHpy_A} = \mathrm{THpy_A}/\mathrm{Hpy_A^w} \quad (4)$$

because rHpy expresses THpy relative to the group being totally immersed in water. The quantity rHpy can therefore be used to characterize and rank the degree of hydrophobicity of different microenvironments independent of group size.

The Rekker hydrophobic fragmental constants are negative for hydrophilic fragments and positive for hydrophobic ones. Thus, Hpy can be either positive or negative, while the microenvironment of a titratable group in water is always negative (see last column of Table 1). Evidently, a rHpy value > 1 implies a microenvironment more hydrophilic than water. Analysis of a data set of 204 globular proteins (*33*) found that the average value of rHpy ranged from 0.28 for tyrosine to 0.63 for lysine. Thus, values of rHpy < 0.25 represent microenvironments that are fairly hydrophobic, while values < 0.0 indicate microenvironments that are very hydrophobic. Recent calculations and experimental findings suggest that such microenvironments can shift pK_a values by 3−5 pH units (*39*).

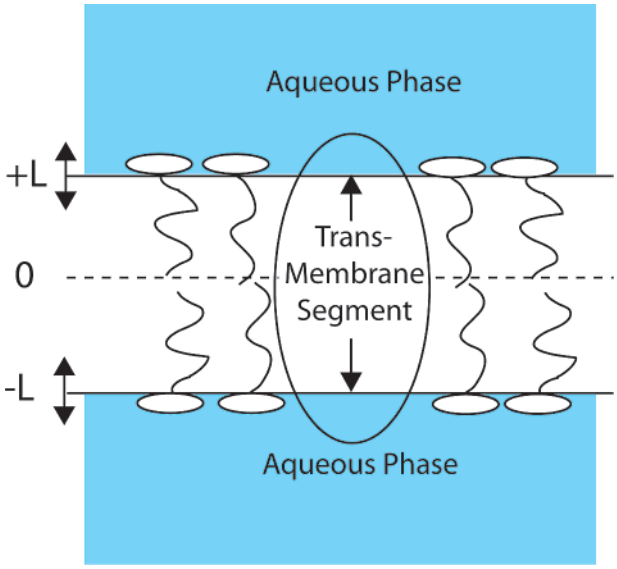

FIGURE 2: Schematic diagram for the calculation of pK_a values for transmembrane proteins. The position of the lipid/water interface is indicated by the L+ and L− planes. The L+ and L− planes lie on the extracellular and cytoplasmic sides of the bilayer, respectively. The definition of the lipid/water interface is the same as in Figure 1.

Hydrophobic Solvent. Unlike globular proteins that are fully immersed in water, some solvent-exposed groups in transmembrane proteins will be exposed to the hydrophobic region of the membrane. The system is represented by a water−lipid−water slab, as shown schematically in Figure 2. Both the water and the lipid regions are treated as continuum solvents. Note that the headgroups are not treated explicitly but are assumed to have the same dielectric properties as the water phase. Because of the polar nature of the headgroups, this is probably a safe assumption. To calculate the contribution from this hydrophobic solvent to the microenvironment, a procedure was used that is similar to that used earlier for water (*30*): Each titratable residue, capped with neutral fragments, is immersed in an octane droplet of radius 20 Å, which is built from an equilibrated box of 126 octane molecules. The droplet consists of about 115−118 octane molecules, and each system comprises around 3000 atoms. The system is heated to 310 K and then equilibrated for 300−400 ps using CHARMM and the PAR22 force field (*40*). From the last 30 ps of the run, 30 structures are extracted, and the microenvironment around the titratable moiety is calculated from each structure. The average from the 30 structures is taken to represent the hydrophobicity, Hpy^o, of the microenvironment around the given residue in octane; the results are given in Table 1.

In addition to the octane values, Table 1 gives the corresponding results for the residues immersed in water, Hpy^w, and it is seen that there is a large difference between the octane and the water values, and the water values are larger in magnitude. The reasons for this are that the Rekker fragmental hydrophobic constant of a water molecule is about twice as large in magnitude as that of a CH_2 or CH_3 group and that water packs more efficiently around the residue than octane. The calculation of rHpy is still based on water, i.e., rHpy = THpy/Hpy^w so that eq 1 can be used for calculating the pK_a values of groups embedded in the hydrophobic portion of the membrane.

Computational Details. The same protocol as reported previously (*30*, *33*) was used for calculating the pK_a values in rhodopsin. In particular, all crystal water molecules were removed and hydrogen atoms were added using the HBUILD option in CHARMM (*41*) but no additional minimization was carried out. The calculations are based on the crystal structures 1HZX (*42*) and 1L9H (*43*). These structures are missing residues in loop C3 (236−240) and in the C terminus (331−333). The two small segments were completed in the structure 1HZX using a protocol designed for the prediction of loop conformations in globular and transmembrane proteins. The protocol has been shown to give reasonable results and has been reported elsewhere (*44*, *45*).

The parameterization is the same as used previously (*30*), although it was derived using experimental pK_a values in globular proteins. No attempt was made to optimize the method for transmembrane proteins because of the lack of quantitative experimental data; therefore, the calculated pK_a values should be interpreted as qualitative indicators of the pK_a shifts. The reference pK_a(s) values used were as follows: N-term, 7.5; C-term, 3.8; His, 6.3; Glu, 4.4; Asp, 4.0; Tyr, 10.0; Lys, 10.4; and Arg, 12.0. Partial charges are taken from the PAR19 force field (*41*) for the standard forms of the amino acid residues; otherwise, they are taken from PAR22 (*40*, *46*). The charges for retinal were kindly provided by K. Schulten.

To carry out the pK_a calculations, the center of mass (CM) of the protein was positioned at the origin of the Cartesian coordinate system and its principal axis was oriented parallel to the membrane normal (*z*-axis). The resulting orientation of the protein compares very well with the orientation of Baldwin's model (*47*) based on electron cryomicroscopy experiments (*48*). In our model, the extent of the hydrophobic region in which the protein is embedded is delimited by the position of two planes, termed L+ (extracellular plane) and L− (cytoplasmic plane), that are perpendicular to the membrane normal, as shown in Figure 2. Note that in this way, the lipid/water interface is defined as the border between the hydrophobic region of the lipids and the polar headgroups. The positions of the two planes are independent and given as input to the program (http://physbio.mssm.edu/~mehler). In this manner, the hydrophobic limits of the slab can be modified easily.

To calculate THpy for titratable residues in transmembrane proteins, the octane or water values are used depending on the phase in which the residue is immersed. The choice of the phase in which the residue is buried in depends on the location of the CM of its titratable moiety relative to the slab as it is defined above (see Figure 2). Thus, if the CM is in the lipid slab (within the region delimited by the L+ and L− planes), the entire titratable group is assumed to be in this phase and similarly for the water regions (outside the same planes).

RESULTS AND DISCUSSION

Rhodopsin was placed in a hydrophobic slab, delimited by two planes L+ and L−, as described in the Materials and Methods section (Figure 2). As a starting point for the pK_a calculations, we chose to place the L+ plane (extracellular side) and the L− plane (intracellular side) each at 15 Å from the center of the bilayer ($z = 0$). This choice is consistent with some estimates (30 Å) for the thickness of the hydrophobic patch of rhodopsin (*28*, *49*). (Note that the pK_a of a given group does not depend on the thickness of the hydrophobic patch but on its actual position relative to L+ or L−.)

Table 2: Structure Dependence of pK_a Values[a]

residue	structure	BF[b]	pK_a	Ave[c]	rHpy	w^{int} [d]	$\alpha\Delta w^{tr}$ [d]	locus[e]
His65	1L9H	0.99	7.7	7.1	0.21	−2.79	0.98	C1
	1HXZ	0.98	6.6		0.15	−2.56	2.13	
Arg177	1L9H	0.86	12.2	11.5	0.48	−2.11	1.85	E2
	1HXZ	0.87	10.8		0.49	−0.25	1.86	
Glu181	1L9H	1.00	7.7	8.5	0.08	0.54	3.94	E2
	1HXZ	1.00	9.3		0.00	0.88	5.91	
Glu239	1L9H	0.93	4.8	4.0	0.06	−3.18	3.68	C3
	1HXZ	0.97	3.2		0.10	−2.47	0.62	

[a] The values are obtained with the hydrophobic/aqueous interface placed at ±15 Å. [b] BF is the buried fraction. [c] Ave is the average pK_a value. [d] Energies are in kcal/mol. [e] Position of the residue (C, cytoplasmic loops; E, extracellular loops).

Structure Dependence of the Calculated pK_a. As has been noted previously (*50*−*52*), a better representation of the experimental pK_a values can be obtained by averaging the calculated values from different structures. Thus, the pK_a values of the titratable residues (Arg, Lys, His, Asp, and Glu) in the dark state of rhodopsin were calculated using the crystal structures 1L9H (*43*) and 1HZX (*42*). (Tyrosine residues were excluded because none titrated below a pK_a value of 10.0 and therefore were outside of the pH range of interest.)

The root-mean-square differences between the two crystal structures are only 0.35 and 0.50 Å for Cα atoms and all heavy atoms, respectively. Comparison of the calculated pK_a values using 1L9H vs those calculated using 1HZX showed that out of 48 titratable groups, only four residues had a pK_a shift larger than 1 pK_a unit (Table 2, a complete list of the calculated pK_a is given as Supporting Information). The four residues (H65, R177, E181, and E239) that present somewhat significant differences are located in extracellular or cytoplasmic loops. These are generally the most mobile parts of a protein, so that the greater variability in the calculated pK_a values is not so surprising. Moreover, the four residues are buried in the protein interior and their pK_a is thus likely to be more sensitive to small changes in conformation of the nearby protein environment. Indeed, small conformational changes could lead to changes in the hydrophobicity of the microenvironment and/or electrostatic interaction that could modify both the transfer energy ($\alpha\Delta w^{tr}$) term and the electrostatic interaction energy (w^{int}) term in eq 1.

Nevertheless, the calculated pK_a values of most titratable groups were not very different in both structures, and with the exception of H65 whose calculated pK_a is 6.6 in 1HZX and 7.7 in 1L9H, the pK_a differences between the two structures did not change the predicted protonation state of the corresponding residues at physiological pH (7.0). Thus, the calculated pK_a values indicate that at physiological pH (7.0) H65 is present in both protonated and deprotonated forms in substantial concentration, whereas E181 is neutral, and R177 and E239 are charged. In the next section, we examine the pK_a values and the corresponding protonation state, at physiological pH, of several key residues in rhodopsin.

Table 3: Calculated pK_a Values and Observed Protonation States in Rhodopsin

residue	pK_a[a] (calcd)	charge state (exp.)[b]	exp pH	refs
Asp83	6.1	N	5.5	*18*, *53*
Glu113	4.3	C	5.5	*12*
Glu122	9.2	N	5.5	*18*
Glu134	5.3	C	7.1	*19*
Arg135	10.2	C	5.6−7.9	*20*
Glu181	8.5	N	6.5, 6.8	*14*, *54*
PSB296	11.0	C	pK_a > 12	*3*

[a] Average pK_a values obtained from the two crystal structures. [b] N, neutral; C, charged.

Comparison with Experiment. Although no quantitative experimental data have been reported for the pK_a of titratable groups in rhodopsin, the protonation states of several titratable residues at, or near, physiological pH have been determined by FTIR difference spectroscopy (*18*, *19*, *53*) and fluorescence spectroscopy experiments (*14*, *54*) combined with site-directed mutagenesis. Most of these are acidic residues, and the qualitative experimental results suggest that the pK_a values of some of them are strongly shifted in rhodopsin from their values in aqueous solution. The results of the calculations and the experimental observations are given in Table 3.

Overall, comparison of the predicted and experimentally deduced protonation states at physiological pH shows good agreement. The highly hydrophobic environment (rHpy = −0.40) surrounding E122 leads to a pK_a value of 9.2, which supports the experimental finding that this residue is protonated at physiological pH. For the Schiff base (PSB296), higher pK_a values have been suggested in some reports (*55*), but the value found here certainly is in agreement with the observed protonation state. Its counterion (E113) is also found charged (pK_a = 4.4) at physiological pH. In the same way in the salt bridge E134/R135, both residues are found to be charged. The pK_a value of E181 indicates that it is protonated. This is in agreement with its experimentally predicted protonation state (*14*, *54*). It should be noted that a recent study based on molecular dynamics simulations of rhodopsin predicts that E181 should be charged because its environment is structurally unstable during the simulation when this residue is protonated (*56*). However, we have found that the environment of a neutral E181 residue is stable after a full set of internal water molecules was predicted and taken into account for the molecular dynamics simulation (Periole et al. Unpublished results). Finally, the pK_a value of D83 (pK_a = 6.0) would suggest that at physiological pH it is primarily deprotonated. This result is in contrast with the experimental finding (*18*, *53*). However, it is noteworthy that the corresponding experiment (*18*) was not carried out at physiological pH but under slightly acidic conditions (pH = 5.5), at which our calculations also predict it to be protonated.

Effect of Change in Solvent on the pK_a Value of E134. To evaluate the effect of moving the lipid/water interface, the planes L+ and L− in Figure 2 were shifted by up to 4 Å in both directions. Table 4 lists all of the titratable residues (R69, E134, R135, E181, R252, and R314) for which the solvent environment changes from being water to lipid or vice versa, as the L+ and L− are moved. E181 is completely buried, and its pK_a is not affected by the change in solvent environment (Table 4). The degree of solvent exposure for the other residues ranges from only 5 to 49%. However, because the quantitative contribution of the solvent to the hydrophobicity of the microenvironment is large (see Table 1), even a small degree of exposure will have a substantial effect when the solvent changes from hydrophilic to hydrophobic. Indeed, Table 4 shows that the main source of the altered pK_a values is the transfer energy ($\alpha\Delta w^{tr}$) that becomes much larger when the titratable residue is immersed in a lipid (hydrophobic) environment. The response of the pK_a values to changes in solvent properties is most dramatically illustrated by R252 and R314, because of their high solvent exposure (49 and 43%, respectively). For these two residues, the change of the solvent environment from water to lipid results in a large shift in the value of their relative hydrophobicity (rHpy) from average hydrophilic (0.58 and 0.50, respectively) to extremely hydrophobic (−0.22 and −0.19, respectively) leading to a concomitant large change in their transfer energy (from 0.08 to 6.41 kcal/mol for R252 and from 0.04 to 6.40 kcal/mol for R314).

Table 4: Shifts in pK_a Values of Residues for Which There Is a Change in Solvent Environment

residue	BF[a]	solvent[b]	pK_a[c]	rHpy	w^{int} [d]	$\alpha\Delta w^{tr}$ [d]
Arg69	0.75	W	13.3	0.56	−2.29	0.11
		L	12.7	0.15	−3.14	2.14
Glu134	0.91	W	5.3	0.12	−0.56	1.81
		L	8.0	0.00	−0.92	5.90
Arg135	0.95	W	10.1	0.08	−1.50	4.08
		L	8.3	0.01	−1.31	6.41
Glu181	1.00	W	7.7	0.08	0.54	3.94
		L	7.7	0.08	0.54	3.94
Arg252	0.51	W	13.3	0.58	−2.22	0.08
		L	9.1	−0.22	−2.43	6.41
Arg314	0.57	W	12.8	0.50	−1.16	0.04
		L	8.3	−0.19	−1.36	6.40

[a] Buried fraction. [b] W, water; L, lipid. [c] pK_a values obtained from the 1L9H (*43*) crystal structure only. [d] Energies are in kcal/mol.

Interestingly, all of the titratable residues that show a large response to the change in the solvent environment are located on the cytoplasmic side of rhodopsin (Table 4). Remarkably, only for E134 would the shift in pK_a value lead to a change in protonation state at physiological pH. This observation makes it tempting to assign a special role to the placement of E134 near the lipid/water interface on the cytoplasmic side. As noted in the Introduction, the triad D(E)RY is highly conserved in GPCRs and neutralization of the glutamate has been suggested as part of the activation process (*11*, *17*−*21*, *57*, *58*). Here, it is seen that the E134 protonation state is extremely sensitive to changes of its microenvironment.

CONCLUSIONS

The pK_a values of all titratable residues in rhodopsin have been calculated using a modified version of the MM-SCP approach (*33*) that takes into account the hydrophobic membrane surrounding the protein. The results are in good agreement with the experimental data on the protonation states of some residues in rhodopsin (Table 3). Thus, we have predicted that E122 and E181 are protonated at physiological pH. Under these same conditions, the residues in the E113/PSB296 and E134/R135 salt bridges are charged. E83 is predicted to be charged at pH 7, and its pK_a (6.0) indicates that it would be protonated at pH 5.5 as found

experimentally (*18*). The pK_a values of the other residues (see the full list given as Supporting Information) do not present any remarkable behavior.

The results show that when the solvent contribution to the microenvironment of an ionizable residue changes from strongly hydrophilic (water) to hydrophobic (lipid) large shifts in the pK_a value of this residue can occur even when the degree of solvent exposure is small (Table 4). Most remarkably, the results show that among all titratable residues in rhodopsin E134 occupies a strategic position near the lipid/water interface that makes its pK_a and therefore its ability to change its protonation state particularly sensitive to changes in the microenvironment. This finding, which emphasizes the special sensitivity of E134's protonation state to its solvent environment, lends further support to experimental studies that have suggested that E134 is involved in the activation mechanism of rhodopsin through a change of its protonation state between rhodopsin and MII (*11*, *17*−*21*, *57*, *58*). The special role of E134 is further emphasized by its conservation in GPCRs.

To model the change in solvent environment that resulted in a shift of pK_a value for E134, it was assumed that the water/lipid interface moved to different positions relative to the protein. This was achieved by simply changing the position of the L− and L+ plane (Figure 2). There is experimental evidence that indicates that such a mechanism could play a role in the activation of rhodopsin. Notably, surface plasmon resonance measurements have established that the membrane embedding rhodopsin thickens in response to an elongation of the protein upon its activation (*59*, *60*). The protonation state of E134 would only be affected by these responses to activation if they concomitantly cause a shift in the environment of E134 from water to lipid. In addition, membrane composition that has been shown to affect the MI/MII equilibrium (*61*, *62*) has also been shown to affect the thickness of the membrane (*63*). Our results suggest that changes in membrane composition could be perturbing the formation of MII by indirectly or directly affecting the ability of E134 to become protonated. The model of "hydrophobic mismatch" (*49*, *64*−*66*) where both the protein and the embedding membrane respond to the forces introduced by a difference in their hydrophobic patches, may indeed result in a displacement of the lipid/water interface around rhodopsin.

Other mechanisms exist that could affect the microenvironment of E134. These include conformational changes within rhodopsin upon activation (*67*). Notably, it has been suggested that the protonation of E134 could be linked to the transfer of its carboxylic acid moiety from a polar to a nonpolar environment (*19*). This could occur as a consequence of changes in lipid−protein interactions resulting from changes in receptor conformation associated with activation and Gt complexation (*19*). Most likely, the observed change in protonation state of E134 between rhodopsin and the MII state (*11*, *19*) is the result of a complex combination of all of these events. Nevertheless, the present results emphasize that the position of E134 at the cytoplasmic lipid/water interface is likely to be a strategic element in the mechanism of rhodopsin activation because it makes this residue particularly amenable to change its protonation state.

ACKNOWLEDGMENT

We thank Dr. Thomas Huber for helpful discussions. Computational support was provided by the National Science Foundation Terascale Computing System at the Pittsburgh Supercomputing Center. We also acknowledge access to the computer facilities at the Institute of Computational Biomedicine (ICB) of the Mount Sinai Medical Center.

SUPPORTING INFORMATION AVAILABLE

Table of the calculated pK_a values for all titratable residues in rhodopsin (PDB entries 1L9H and 1HZX). This material is available free of charge via the Internet at http://pubs.acs.org.

REFERENCES

1. Palczewski, K., Kumasaka, T., Hori, T., Behnke, C. A., Motoshima, H., Fox, B. A., Le Trong, I., Teller, D. C., Okada, T., Stenkamp, R. E., Yamamoto, M., and Miyano, M. (2000) *Science 289*, 739−745.
2. Menon, S. T., Han, M., and Sakmar, T. P. (2001) *Physiol. Rev. 81*, 1659−1688.
3. Sakmar, T. P., Menon, S. T., Marin, E. P., and Awad, E. S. (2002) *Annu. Rev. Biophys. Biomol. Struct. 31*, 443−484.
4. Okada, T., Ernst, O. P., Palczewski, K., and Hofmann, K. P. (2001) *Trends Biochem. Sci. 26*, 318−324.
5. Pan, D., Ganim, Z., Kim, J. E., Verhoeven, M. A., Lugtenburg, J., and Mathies, R. A. (2002) *J. Am. Chem. Soc. 124*, 4857−4864.
6. Siebert, F. (1995) *Isr. J. Chem. 35*, 309−323.
7. Farrens, D. L., Altenbach, C., Yang, K., Hubbell, W. L., and Khorana, H. G. (1996) *Science 274*, 768−770.
8. Parkes, J. H., and Liebman, P. A. (1984) *Biochemistry 23*, 5054−5061.
9. Gibson, S. K., Parkes, J. H., and Liebman, P. A. (1999) *Biochemistry 38*, 11103−11114.
10. Arnis, S., and Hofmann, K. P. (1993) *Proc. Natl. Acad. Sci. U.S.A. 90*, 7849−7853.
11. Arnis, S., Fahmy, K., Hofmann, K. P., and Sakmar, T. P. (1994) *J. Biol. Chem. 269*, 23879−23881.
12. Jager, F., Fahmy, K., Sakmar, T. P., and Siebert, F. (1994) *Biochemistry 33*, 10878−10882.
13. Sakmar, T. P., Franke, R. R., and Khorana, H. G. (1989) *Proc. Natl. Acad. Sci. U.S.A. 86*, 8309−8313.
14. Yan, E. C., Kazmi, M. A., Ganim, Z., Hou, J. M., Pan, D., Chang, B. S., Sakmar, T. P., and Mathies, R. A. (2003) *Proc. Natl. Acad. Sci. U.S.A. 100*, 9262−9267.
15. DeCaluwe, G. L., Bovee-Geurts, P. H., Rath, P., Rothschild, K. J., and de Grip, W. J. (1995) *Biophys. Chem. 56*, 79−87.
16. Probst, W. C., Snyder, L. A., Schuster, D. I., Brosius, J., and Sealfon, S. C. (1992) *DNA Cell Biol. 11*, 1−20.
17. Franke, R. R., Sakmar, T. P., Graham, R. M., and Khorana, H. G. (1992) *J. Biol. Chem. 267*, 14767−14774.
18. Fahmy, K., Jager, F., Beck, M., Zvyaga, T. A., Sakmar, T. P., and Siebert, F. (1993) *Proc. Natl. Acad. Sci. U.S.A. 90*, 10206−10210.
19. Fahmy, K., Sakmar, T. P., and Siebert, F. (2000) *Biochemistry 39*, 10607−10612.
20. Weitz, C. J., and Nathans, J. (1993) *Biochemistry 32*, 14176−14182.
21. Kim, J. M., Altenbach, C., Thurmond, R. L., Khorana, H. G., and Hubbell, W. L. (1997) *Proc. Natl. Acad. Sci. U.S.A. 94*, 14273−14278.
22. Scheer, A., Fanelli, F., Costa, T., De Benedetti, P. G., and Cotecchia, S. (1996) *EMBO J. 15*, 3566−3578.
23. Scheer, A., Fanelli, F., Costa, T., De Benedetti, P. G., and Cotecchia, S. (1997) *Proc. Natl. Acad. Sci. U.S.A. 94*, 808−813.
24. Arora, K. K., Cheng, Z., and Catt, K. J. (1997) *Mol. Endocrinol. 11*, 1203−1212.
25. Morin, D., Cotte, N., Balestre, M. N., Mouillac, B., Manning, M., Breton, C., and Barberis, C. (1998) *FEBS Lett. 441*, 470−475.
26. Ballesteros, J. A., Kitanovic, S., Guarnieri, F., Davies, P., Fromme, B. J., Konvicka, K., Chi, L., Millar, R., Davidson, J. S., Weinstein, H., and Sealfon, S. C. (1998) *J. Biol. Chem. 273*, 10445−10453.

27. Farahbakhsh, Z. T., Ridge, K. D., Khorana, H. G., and Hubbell, W. L. (1995) *Biochemistry 34*, 8812−8819.
28. Stenkamp, R. E., Filipek, S., Driessen, C. A., Teller, D. C., and Palczewski, K. (2002) *Biochim. Biophys. Acta 1565*, 168−182.
29. Mehler, E. L. (1996) *J. Phys. Chem. 100*, 16006−16018.
30. Mehler, E. L., and Guarnieri, F. (1999) *Biophys. J. 77*, 3−22.
31. Warshel, A. (1981) *Biochemistry 20*, 3167−3177.
32. Bashford, D., and Karplus, M. (1990) *Biochemistry 29*, 10219−10225.
33. Mehler, E. L., Fuxreiter, M., Simon, I., and Garcia-Moreno E. B. (2002) *Proteins 48*, 283.
34. Ponnuswamy, P. K., Prabhakaran, M., and Manavalan, P. (1980) *Biochim. Biophys. Acta 623*, 301−316.
35. Bowie, J. U., Luthy, R., and Eisenberg, D. (1991) *Science 253*, 164−170.
36. Kleiger, G., Beamer, L. J., Grothe, R., Mallick, P., and Eisenberg, D. (2000) *J. Mol. Biol. 299*, 1019−1034.
37. Rekker, R. F. (1979) *Eur. J. Med. Chem. 14*, 479−488.
38. Rekker, R. F. (1977) *The Hydrophobic Fragmental Constant*, Vol. 1, Elsevier, Amsterdam.
39. Schutz, C. N., and Warshel, A. (2001) *Proteins 44*, 400−417.
40. MacKerell, A. D., Jr., Bashford, D., Bellott, M., Dunbrack, R. L., Jr., Evanseck, J. D., Field, M. J., Fischer, S., Gao, J., Guo, H., Ha, S., Joseph-McCarthy, D., Kuchnir, L., Kuczera, K., Lau, F. T. K., Mattos, C., Michnick, S., Ngo, T., Nguyen, D. T., Prodhom, B., Reiher, W. E., III, Roux, B., Schlenkrich, M., Smith, J. C., Stote, R., Straub, J., Watanabe, M., Wiorkiewicz-Kuczera, J., Yin, D., and Karplus, M. (1998) *J. Phys. Chem. B 102*, 3586−3616.
41. Brooks, B. R., Bruccoleri, R. E., Olafson, B. D., States, D. J., Swaminathan, S., and Karplus, M. (1983) *J. Comput. Chem. 4*, 187−217.
42. Teller, D. C., Okada, T., Behnke, C. A., Palczewski, K., and Stenkamp, R. E. (2001) *Biochemistry 40*, 7761−7772.
43. Okada, T., Fujiyoshi, Y., Silow, M., Navarro, J., Landau, E. M., and Shichida, Y. (2002) *Proc. Natl. Acad. Sci. U.S.A. 99*, 5982−5987.
44. Hassan, S. A., Mehler, E. L., and Weinstein, H. (2002) in *Lecture Notes in Computational Science and Engineering* (Hark, K., and Schlick, T., Eds.) pp 197−231, Springer-Verlag, Ag., New York.
45. Mehler, E. L., Periole, X., Hassan, S. A., and Weinstein, H. (2002) *J. Comput.-Aided Mol. Des. 16*, 841−853.
46. MacKerell, A. D. J., Bashfod, D., Bellot, M., Dunbrack, R. L. J., Field, M. J., Fischer, S., Gao, J., Guo, H., Ha, S., Joseph, D., Kuchnir, L., Kuczera, K., Lau, F. T. K., Mattos, C., Michnick, S., Ngo, T., Nguyen, D. T., Prodhom, B., Roux, B., Schlenkrich, M., Smith, J., Stote, R., Straub, J., Wiorkiewicz-Kuczera, J., and Karplus, M. (1992) *Biophys. J. 6*, A143.
47. Baldwin, J. M., Schertler, G. F., and Unger, V. M. (1997) *J. Mol. Biol. 272*, 144−164.
48. Unger, V. M., Hargrave, P. A., Baldwin, J. M., and Schertler, G. F. (1997) *Nature 389*, 203−206.
49. Dumas, F., Lebrun, M. C., and Tocanne, J. F. (1999) *FEBS Lett. 458*, 271−277.
50. van Vlijmen, H. W. T., Schaefer, M., and Karplus, M. (1998) *Proteins 33*, 145−158.
51. Georgescu, R. E., Alexov, E. G., and Gunner, M. R. (2002) *Biophys. J. 83*, 1731−1748.
52. Alexov, E. G., and Gunner, M. R. (1997) *Biophys. J. 74*, 2075−2093.
53. Rath, P., DeCaluwe, L. L., Bovee-Geurts, P. H., DeGrip, W. J., and Rothschild, K. J. (1993) *Biochemistry 32*, 10277−10282.
54. Yan, E. C., Kazmi, M. A., De, S., Chang, B. S., Seibert, C., Marin, E. P., Mathies, R. A., and Sakmar, T. P. (2002) *Biochemistry 41*, 3620−3627.
55. Steinberg, G., Ottolenghi, M., and Sheves, M. (1993) *Biophys. J. 64*, 1499−1502.
56. Rohrig, U. F., Guidoni, L., and Rothlisberger, U. (2002) *Biochemistry 41*, 10799−10809.
57. Cohen, G. B., Yang, T., Robinson, P. R., and Oprian, D. D. (1993) *Biochemistry 32*, 6111−6115.
58. Acharya, S., and Karnik, S. S. (1996) *J. Biol. Chem. 271*, 25406−25411.
59. Salamon, Z., Wang, Y., Brown, M. F., Macleod, H. A., and Tollin, G. (1994) *Biochemistry 33*, 13706−13711.
60. Salamon, Z., Brown, M. F., and Tollin, G. (1999) *Trends Biochem. Sci. 24*, 213−219.
61. Brown, M. F. (1994) *Chem. Phys. Lipids 73*, 159−180.
62. Botelho, A. V., Gibson, N. J., Thurmond, R. L., Wang, Y., and Brown, M. F. (2002) *Biochemistry 41*, 6354−6368.
63. Separovic, F., and Gawrisch, K. (1996) *Biophys. J. 71*, 274−282.
64. Mouritsen, O. G., and Bloom, M. (1984) *Biophys. J. 46*, 141−153.
65. Killian, J. A. (1998) *Biochim. Biophys. Acta 1376*, 401−415.
66. Killian, J. A. (2003) *FEBS Lett. 555*, 134−138.
67. Hubbell, W. L., Altenbach, C., Hubbell, C. M., and Khorana, H. G. (2003) *Adv. Protein Chem. 63*, 243−290.
68. Altenbach, C., Yang, K., Farrens, D. L., Farahbakhsh, Z. T., Khorana, H. G., Hubbell, W. L., and Killian, J. A. (1996) *Biochemistry 35*, 12470−12478.
69. Altenbach, C., Klein-Seetharaman, J., Hwa, J., Khorana, H. G., Hubbell, W. L., Cai, K., Yang, K., Farrens, D. L., Farahbakhsh, Z. T., and Killian, J. A. (1999) *Biochemistry 38*, 7945−7949.
70. Altenbach, C., Cai, K., Khorana, H. G., Hubbell, W. L., Yang, K., Farrens, D. L., Farahbakhsh, Z. T., and Killian, J. A. (1999) *Biochemistry 38*, 7931−7937.

BI049949E